View metadata, citation and similar papers at core.ac.uk
brought to you by CORE
provided by University of Huddersfield Repository

Development of a spatially dispersed short-coherence interferometry sensor using diffraction grating orders

MOTHANA A. HASSAN,[1,2,*] HAYDN MARTIN,[2] AND XIANG JIANG[2]

[1]*Laser and optoelectronics Engineering Department, University of Technology, Baghdad, Iraq*
[2]*EPSRC Future Metrology Hub, University of Huddersfield, UK*
**Corresponding author: dr.mothana.hassan@gmail.com*

Received XX Month XXXX; revised XX Month, XXXX; accepted XX Month XXXX; posted XX Month XXXX (Doc. ID XXXXX); published XX Month XXXX

Modern manufacturing processes can achieve good throughput by requiring that manufactured products be screened by better quality control exercised at a quicker rate. This trend in the quality control of manufactured products increases the need for process-oriented precision metrology capable of performing faster inspections and yielding valuable feedback to the manufacturing system. This paper presents a spatially dispersed short-coherence interferometry sensor using diffraction orders of the zeroth and first-order for a diffraction grating has been introduced as a new compact system configuration for surface profile measurement. In this modified design, the diffraction grating acts as the beam splitter/combiner. Diffractions for the zeroth and first-orders are represented by the reference and measurement arms, respectively, of a Michelson interferometer, which reduces the optical path length. This innovative design has been proven effective for determining the step-height repeatability in the sensor range from 27 nm to 22 nm for profiles spanning the step-heights of the tested specimens. **© 2017 Optical Society of America**

OCIS codes: *(050.5080) Phase shift, (070.0070) Fourier optics and signal processing, (120.3180) Interferometry, (120.6200) Spectrometers and spectroscopic instrumentation, (170.4500) Optical coherence tomography, (170.5810) Scanning microscopy, (240.0240) Optics at surfaces, (240.6700) Surfaces.*

http://dx.doi.org/10.1364/AO.99.099999

1. INTRODUCTION

Embedded metrology combines the metrology of industrial machine platforms with measurements performed without removing tested materials from the workplace. In addition, embedded metrology represents the specialised uses of instrument control of precise, online measurement tools capable of fast-rate data collection in ways immune to environmental noise. Many researchers have reported investigations of inline and online surface metrology processes performed in many locations around the world over the last 30 years. For the most part, the methods used during the manufacturing inline and online processes are based on the concepts of assessing speckles or employing diffuse-light techniques; these techniques enable the extraction of surface textures with microscale properties [1–4]. The main difficulty arising with these systems is that they cannot detect more information from the submicroscale surface features of the sample under testing conditions [5,6]. However, the advantages of optical profilometry lie its capacity for performing noncontact measurements of delicate surfaces, enhanced scanning range and high data-collection rate [7,8].

Any practical measurement method must satisfy several key requirements to support successful uses of embedded metrology in manufacturing platforms: noncontact measurements, high-speed operations, compact systems and probes and insensitivity to environmental noise. However, several applications are not suitable for analysing defects on moving substrates because such approaches require moving the objective lens. Dynamic applications present problems in performing identifications during roll-to-roll production; it is often sufficient to evaluate sample information only inline because the second lateral measurement axis is supplied by the movement of the substrate. However, achieving high precision is complicated by the type of profile algorithm the application uses to extract the surface characterisation from the sample [9,10]. Improvements in online techniques for surface profile measurement will prove beneficial by enabling many high-precision and ultraprecise manufacturing applications and reducing their costs of operation.

Currently available optical metrology sensors tend to be expensive and bulky and to operate at slow detection speeds. The inherent benefit of optical methods for implementing embedded surface topography measurements in manufacturing is their potential for use as sensors that provide fast measurements without surface contact. The speed limitations and large size of the traditional optical instruments have inspired researchers to investigate a new approach to overcome these limitations. Single-shot interference-based measurements require that all necessary data be captured in one recorded interferogram pattern [11]. Several authors have demonstrated instruments based on the single-shot interferometry method for reducing the effects of noise and vibrations. However, some of these applications used non-standard components, such as the

micropolariser-array phase-shifting method [12–15]. Several single-shot measurement instruments and techniques, such as frequency-resolved optical gatings and spectral-phase interferometry for direct electric-field reconstruction, are powerful techniques for acquiring measurements in real time with high resolution. Nevertheless, these techniques are based on the stroboscopic measurement method; thus, they are unsuitable for real-time measurements. Moreover, these methods cannot obtain repetitive measurements of complex physical samples [16–18]. Therefore, a method is needed for evaluating the modulation frequency; such methods are based on a single-shot line-scanning measurement technique: Fourier transform profilometry (FTP). FTP has been applied to perform rapid extractions of the instantaneous phase from a modulation interferogram pattern [19–22].

The viability and efficacy of spatially dispersed short-coherence interferometry (SDSCI) sensor is made possible with the implementation of a broadband dispersed measurement interferometer. It produces line/profile dispersion using a single grating in the measurement arm (dispersive optical probe). This is the first interferometer implemented and it can measure surface topographies on a sub-micron scale. It achieves this via line scanning by employing of wavelength division multiplexing with a dispersive optical probe. The interferometric technique is able to provide instantaneous wide profile measurements at a range of up to 2 mm by employing a 10X objective scan lens, rather than any conventional scanning mechanism. Consequently, this technique has the potential to be used for single-shot measurement application, whereby the speed is regulated only by a single exposure time of spectrometer camera speed. The SDSCI sensor proposed here to implement FTP by using a superluminescent diode (SLD) as a broadband light source. The results were analysed using the FTP method, which involves subtracting the slope of the phase shifts from the interference intensity for each pixel. The SDSCI sensor was rigorously tested using a spectrally resolved broadband interferogram. This gives a basis for determining the surface profiles in the nanoscale range. The SDSCI sensor features a compact interior arrangement. This is in response to some of the challenges already identified in the paper. The SDSCI sensor operates at the nanometre scale when measuring surface step height. Moreover, this paper reports that this SDSCI sensor represents progress towards the development of a novel high-precision compact device usable in embedded surface and dimensional metrology applications requiring SDSCI sensor. Two SDSCI layout configurations were used to evaluate the obtained interferogram based on a single-shot profilometry method. The performance of the SDSCI sensor shows it offers enhanced repeatability of operations by reducing the uncommon optical path length (OPL) between the reference and measurement arms of the interferometer.

2. PRINCIPLE OF OPERATION

Investigation of spatially short coherence dispersive interferometry is important for applications to optical metrology inspections based on single-shot line-scanning interferometers. The proposed configuration employs a Michelson interferometer illuminated by an super luminescent diode SLD (Exalos EXS8310-8411) operating at a central wavelength of 820 nm with a broadband of 25 nm as illustrated in Fig. 1. The broadband of the light source is spatially dispersed across the profile on the sample tested using the diffraction grating and objective scan lens (dispersive optical probe). The interferogram is spatially dispersed, and the optical phase is determined simultaneously for each sampled wavelength. This spectrally resolved phase data can be used to perform an interferometric extraction of the surface information topography by taking advantage of the relationship of the topography to an optical path difference in the interferometer. The surface topography information can be obtained from the dispersed profile across the tested sample.

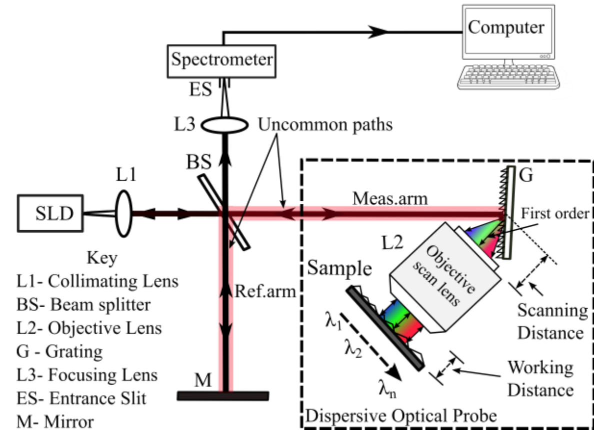

Fig. 1. Previous SDSCI sensor configuration arrangement.

The dispersed encoded profile length is an important factor that depends on several major factors: the numerical aperture NA of the scanning objective lens, the type of grating features and the characterisations of the spectrometer. This paper reports on tests of a new updated configuration for the SDSCI sensor as introduced in the previous paper [20].

The spectrometer output was recorded as the path length in the reference arm was changed incrementally. Each wavelength, as analysed by the spectrometer, was mapped to a single position x along a line on the sample through the action of the dispersive optical probe. Then, the phase of the interferogram pattern at any specific wavelength was a function of the optical path difference (OPD). Thus, the surface height h was obtained at the respective surface position x. The general function of the SDSCI sensor is given by [22]

$$I(x,\lambda) = I_r(\lambda) + I_m(x_\lambda)\cos\phi(x,\lambda). \quad \textbf{(1)}$$

Where $I_r(\lambda)$ and $I_m(x_\lambda)$ are the intensities at the reference and measurement arms, respectively, and ϕ is the phase difference, which is related directly to the surface height h by the expression

$$\phi(x,\lambda) = \frac{4\pi}{\lambda} h_x. \quad \textbf{(2)}$$

The interferogram is a function of the dispersive wavelength; this interferogram is used for determining the phase encoded at a given wavelength. Therefore, the surface-height positions are related to the wavelengths. FTP can be applied to extract the phase from the SDSCI sensor; it offers a distinct benefit over phase shift interferometry (PSI) by enabling the capture of the required phase information in a single-shot measurement. The FTP technique initially required a calibration routine in which background intensity was recorded by blocking the measurement arm. After this step was complete, a single spectral interferogram was captured using the spectrometer interrogation. A fast Fourier transform algorithm was employed to determine the phase. Thus,

$$I(x,\lambda) = I_r(\lambda) + \frac{1}{2} I_m(x_\lambda)\exp[i\phi(x_\lambda)] + \frac{1}{2} I_m(x_\lambda)\exp[-i\phi(x_\lambda)]. \quad \textbf{(3)}$$

The middle term of Eq. (3) can be represented by

$$c(x,\lambda)=\frac{1}{2}I_m(x_\lambda)\exp[i\phi(x_\lambda)]. \quad \textbf{(4)}$$

By applying a discrete Fourier transform (DFT) to Eq. (4), the new equation can be written as

$$I(x,\lambda)=A(\lambda)+C(x_\lambda)+C^*(x_\lambda). \quad \textbf{(5)}$$

Where the term $C^*(x_\lambda)$ represents the complex conjugate of C. After an inverse DFT is applied to the conjugated term in Eq (5), the phase can be retrieved by taking the complex logarithm. Thus,

$$\log\left\{\frac{1}{2}I_m(x_\lambda)\exp[i\phi(x_\lambda)]\right\}=\log\left[\frac{1}{2}I_m(x_\lambda)\right]+i\phi(x_\lambda). \quad \textbf{(6)}$$

The phase is now isolated in the imaginary part, which may be unwrapped, if necessary, using a suitable algorithm [5,19,20].

3. EXPERIMENTAL SETUP

The components and arrangement of the original SDSCI sensor were outlined in the previous section as shown Fig. 1. The new updated compact layout is used throughout this paper as shown in Fig. 2. The light-source beam passed through the beam splitter to the grating in the dispersive optical probe and was projected onto the sample. The dispersive optical probe consisted of an objective scan lens (LSM02-BB, Thorlabs), diffraction grating (GR25-1210, Thorlabs) and the sample undergoing testing (Diamond turned multi-step sample). The dispersed light was reflected from the sample to the optical dispersive probe.

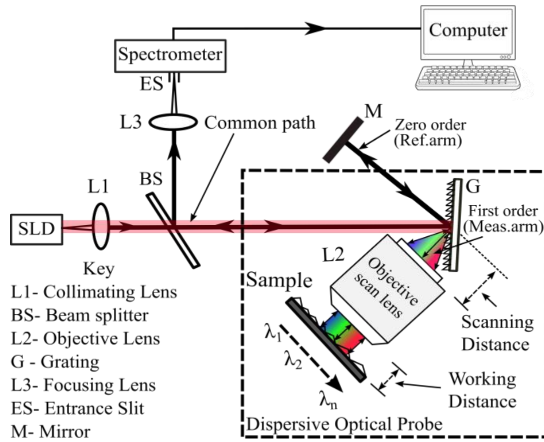

Fig. 2. New SDSCI sensor configuration arrangement using diffraction orders.

The spectral interferogram was obtained from the wavefronts reflected from the sample undergoing testing, and the reference mirror was used for analysis with the compact spectrometer (S150, Solar Laser Systems, Minsk, Belarus). The modified design, rather than using a separate reference beam from the beam splitter, employed as a reference beam the zero order beam reflected from the diffraction grating in the optical probe. Thus, the beam followed a common path along most of its journey until it reached the diffraction grating; there, it underwent diffraction at various angles. Therefore, this arrangement reduced the differences in path lengths to at least one-third of the length of the previous configuration, resulting in a sensor that showed much less sensitivity to environmental effects. This experiment investigated the surface profile by measuring the interferogram pattern generated by the interference between the zero and first order diffraction beams. Figure 2 illustrates the zero and the first-order beams reflecting off the grating forms, serving as the reference and measurement beams, respectively, for the Michelson interferometer configuration. The reference arm (zero-order beam) contains a reflecting mirror, and the measurement arm (first-order beam) propagates its beam through the dispersive probe over the sample. Within a dispersive optical probe, the broadband SLD beam (width 8.3 mm) is angularly dispersed by diffraction grating. The dispersed light is then collimated and focused onto the surface using an objective lens. The objective lens used for SDSCI configuration in this instance was a (LSM02-BB- scan lens, Thorlabs) with an effective focal length of 18 mm. The grating equation is

$$m\lambda=d(\sin\alpha+\sin\beta). \quad \textbf{(7)}$$

Where m is an integer number, d is the grating pitch and λ is the wavelength of the incident light. α , β are the incident and diffracted angles respectively, as illustrated in Fig. 3.

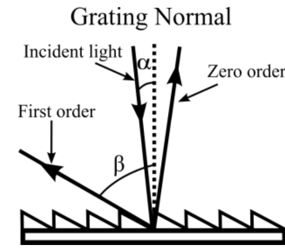

Fig. 3. Utilize angles of diffraction grating orders for the current SDSCI system.

The surface topography information was gathered by introducing the phase at each point on the surface of the reflected light. The lateral scanning direction *x* on the surface was obtained when the broadband of the SLD light was dispersed by the first-order beam through spatial scanning, as shown in Fig. 4 (a, b).

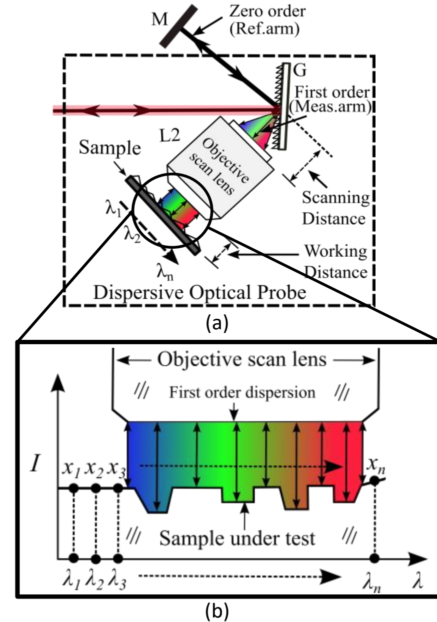

Fig. 4. SDSCI probe and sample details. (a) Dispersive optical probe for the SDSCI sensor. (b) Distribution of wavelengths upon the sample.

The surface scanning range (S) can be determined from the equation

$$S = f\frac{\Delta\lambda}{d\cos\beta}. \quad \textbf{(8)}$$

Where f is the effective focal length of the objective lens, the diffraction grating operates on the first order only, β is the angle of diffraction, d is the density of the grating grooves (1200 L/mm) and $\Delta\lambda$ is the broadband of the light source at 25 nm. The surface topography characterisation is obtained from the phase-detection algorithm through signal processing. Parameters and experimental conditions, similar to those used for previous configurations, were set for the new compact sensor, such that the incident and diffraction angles were 2° and 73.55°, respectively, at the centre SLD wavelength of 820 nm and the angular dispersion was 0.042 rad/nm [20]. Figure 5 shows the calculated scan ranges of different incident angles and it is quite evident that whenever there is a small incident angle, there is a large scanning range to accompany it. Furthermore, the scan range would be approximately linear along the wavelength scan range.

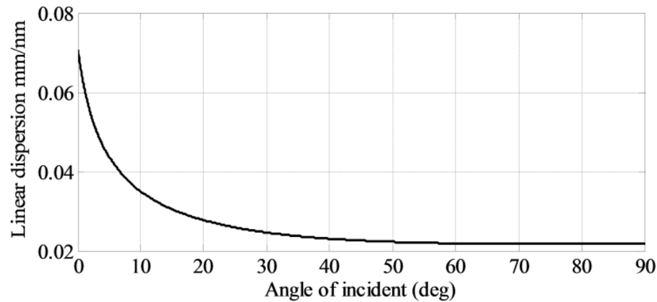

Fig. 5. Linear dispersion vs beam angle of incidence

The scanning range (line profile length) using the objective scan lens was approximately 2 mm as shown in Fig. 6. The beam of SLD is directed to hit the diffraction grating and disperses to the first order and zero orders. The diffraction light first order is collimated using an objective lens. The focal length of the objective scan lens is 18.02 mm. The scan range (line profile length) is one of the most important experimental factors. The scan range has been investigated and verified because it is a critical factor in measuring the entire line profile (system ability) of the sample under test for objective scan lense.

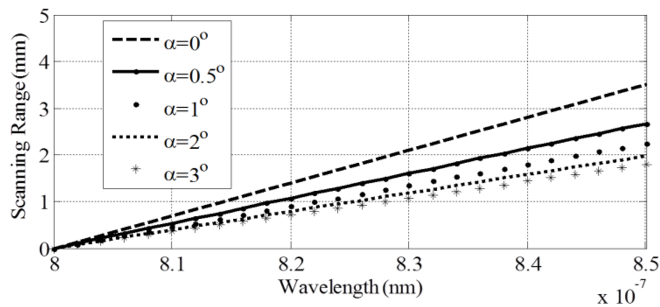

Fig. 6. Scan linearity vs angle of incidence of objective scan lens

The interference pattern produced by the zero and first-order beams is unique, and this can be observed by using a spectrometer CMOS (Complementary Metal-Oxide Semiconductor) camera as shown in Fig. 7. The cross-section of a zero-order beam is about 8 mm, and the first-order (scanning range) beam is 2 mm. However, the difference between the beam sizes does not affect the interference pattern because the dispersed light (first-order) at the dispersive optical probe is reflected back from the test sample to the diffraction grating and thus combines with the zero-order reflected light. In practical terms, the difference in cross-section between the beams (zero and first-order) does not, therefore, affect the interference pattern within the dispersive optical probe concept.

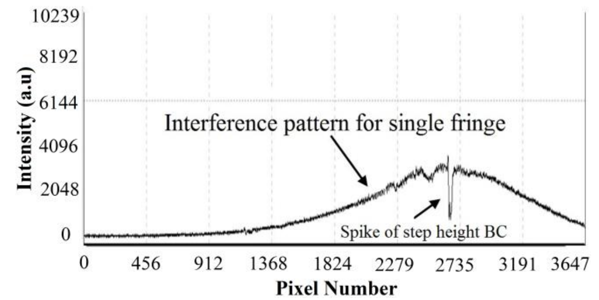

Fig. 7. **Error! No text of specified style in document.**The interferogram pattern of the SDSCI system

The spectrometer S150 is designed to work with the optical fibre type (UV600/660P). It contains a CMOS line array with 3648 pixels and a demonstrable wavelength resolution of 0.06 nm; linear image sensor (Toshiba TDC 1304AP-3648 pixels, pixel size 8μm×200 μm). The spectrometer resolution is a primary focus. The technology for a CMOS allows for small pixel size (~ 4μm) detectors and the readout circuitry directly from each pixel individually. The readout circuitry for each one can be obtained on an individual basis. However, the applicability of the data is restricted by the pixel size of the detector array. The spectral range for spectrometer S150 is between 799 and 840 nm. This was sufficient for the broadband of the SDL light source. The uppermost exposure time is 7.4 ms. This provided time enough to gather the required data. The diffraction grating features 1800 lines/nm and is compatible with a blaze wavelength of 750nm. As this variable also has an impact on spectral resolution, it is worth investigating. Regardless of whether or not the exposure time is suitable, the value of interferometer data is still dependent on a degree of fringe visibility. The fringe visibility for SDSCI sensor has been investigated by changing OPD for micrometre stage at reference arm, and it can be expressed in the form minimum and maximum intensity.

4. EXPERIMENTAL RESULTS AND DISCUSSION

The diamond turned multi-step sample was measured with the new SDSCI sensor configuration. Figure 8 shows the sample surface profile obtained using a PGI stylus instrument (Taylor Hobson Ltd., Leicester, Great Britain) and a proprietary surface analysis software package (Surfstand, University of Huddersfield, Huddersfield, Great Britain). The steps taken to obtain this sample are labelled A through F in the images. After an application of the FTP method to the single-shot measurement extracted the phase and height, the compact SDSCI sensor succeeded in tracking the step height for Step BC. The step-height measurement of the diamond turned multi-step sample was matched with the Taylor Hobson PGI stylus measurement.

The FTP method required between 3 and 30 fringes to resolve the sample. In practice, 10 fringes were used to maintain consistently accurate measurement results. An application of the FTP method with the previous SDSCI sensor layout yielded a measured surface-height profile of the sample for Step BC of approximately 572.09 nm, which agreed with the Taylor Hobson PGI stylus measurement within a deviation of 15.8 nm. In comparison, using the new SDSCI sensor layout produced a step height of approximately 595.8 nm, which was

found to agree with the Taylor Hobson PGI stylus measurement within a deviation of 7.91 nm.

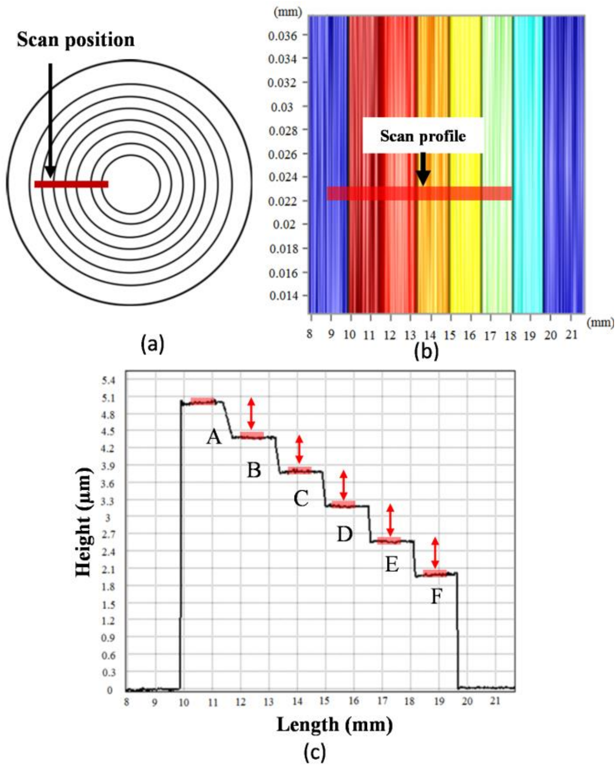

Fig. 8. Step image and surface profile. (a) Diamond-turned multi-stepped concentric circular step. (b) and (c) Surface profiles of the sample obtained using a Taylor Hobson PGI stylus.

These results are depicted in Figs. 9 (a) and 10 (a). The repeatability measurements were performed by taking 100 measurements of the diamond-turned multistep sample using the FTP method under similar experimental conditions. The objective scan lens was used for the probe head.

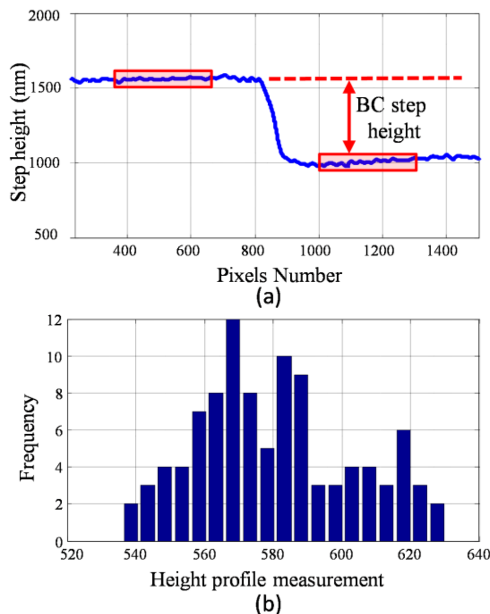

Fig. 9. (a) Step height measurement for diamond turned multi-step sample and using pervious SDSCI configuration, (b) Step height repeatability measurement.

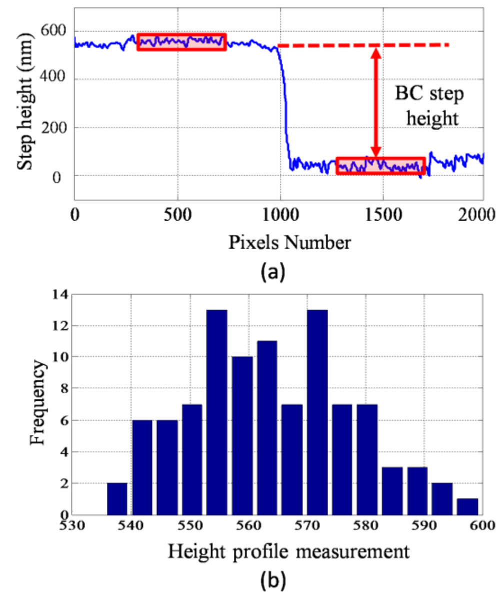

Fig. 10. (a) Step height measurement for diamond turned multi-step sample and using new SDSCI configuration, (b) Step height repeatability measurement

Figures 9 (b) and 10 (b) show the histogram plots for 100 measurements obtained using the FTP method for the previous and new SDSCI sensor layouts, respectively. The sensor system exhibited a measurement repeatability of 22 nm within, two standard deviations (2σ), for the step-height sample. The summary of results in Table 1 shows that the compact SDSCI sensor exhibited better repeatability with small deviation step height measurement than the previous layout of the SDSCI sensor.

Table 1. Comparison between previous and new SDSCI configuration using FTP method

Sample measurement type	SDSCI Layout	Measurement method	Repeatability (nm)	Step height deviation vs PGI (nm)
Diamond turned multi-step	Previous layout	FPP	27	15.8
	New layout	FPP	22	7.91

Consequently, the main focus of this investigation is to substitute a free space SDSCI sensor for the standard optical fibre link sensor in order to meet embedded metrology requirements, as illustrated in Fig. 11. Such sensors are both more compact and robust than conventional solutions, allowing for use in confined or problematic conditions, such as meteorology applications. The compact nature of the sensor also reduces interference from extended optical path lengths, promoting accuracy of measurement. The effectiveness of such sensors under test conditions is likely to reflect their performance in the field, and thus this investigation seeks to demonstrate the feasibility of this simple substitution.

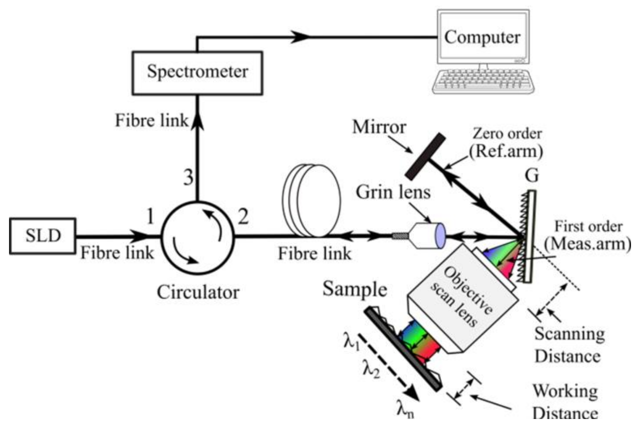

Fig. 11. Initial design for SDSCI optical fibre link sensor.

5. CONCLUSION

A new SDSCI sensor configuration is proposed in order to ensure the sensor is more compact and less sensitive to environmental disturbances. Sensor performance is also enhanced due to the reduction of uncommon optical path lengths between the reference and measurement arms. This modification to previous SDSCI sensor technology ensures that metrology sensor can be made even more compact, which is a major requirement for embedded metrology applications. The step height repeatability of the specimen under test has been measured for 100 readings.

The FTP method is more limited in its ability to resolve surface profiles with high-frequency content in the lateral dimension because of the inability to separate the imposed carrier fringes that are required for accurate FTP analysis. However, FTP remains a potentially useful tool for allowing single-shot measurement utilising SDSCI, allowing applications with dynamic processes or problematic levels of environmental noise such as moving substrates in roll-to-roll manufacturing processes to be carried out. The new SDSC sensor configuration also promises to be easy to convert from a free space variant to optical fibre links where required, removing most of the potential drawbacks.

References

1. X. Jiang, D. Lin, L. Blunt, W. Zhang, and L. Zhang, "Investigation of some critical aspects of on-line surface measurement by a wavelength-division-multiplexing technique," Measurement Science and Technology **17**, 483-487 (2006).
2. R.-S. L. a. G. Y. Tian, "On-line measurement of surface roughness by laser light scattering," IOP Publishing Ltd **1496–1502** (2006).
3. K. Wang, H. Martin, and X. Jiang, "Actively stabilized optical fibre interferometry technique for online/in-process surface measurement," Review of Scientific Instruments **79**, 023109 (2008).
4. K. Creath, "Step height measurement using two-wavelength phase-shifting interferometry," APPLIED OPTICS **Vol. 26, No. 14** (1987).
5. X. Jiang, K. Wang, F. Gao, and H. Muhamedsalih, "Fast surface measurement using wavelength scanning interferometry with compensation of environmental noise," APPLIED OPTICS **Vol. 49, No. 15** (2010).
6. Y.-Y. Cheng and J. C. Wyant, "Two-wavelength phase shifting interferometry," APPLIED OPTICS **23**, 4539-4543 (1984).
7. Z. Sárosi, W. Knapp, A. Kunz, and K. Wegener, Detection of surface defects on sheet metal parts by using one-shot deflectometry in the infrared range (ETH Zurich, IWF, 2010).
8. E. Papastathopoulos, K. Körner, and W. Osten, "Chromatic confocal spectral interferometry," Applied Optics **45**, 8244-8252 (2006).
9. P. C. Lin, P.-C. Sun, L. Zhu, and Y. Fainman, "Single-shot depth-section imaging through chromatic slit-scan confocal microscopy," APPLIED OPTICS **37**, 6764-6770 (1998).
10. I. Dancus, S. T. Popescu, and A. Petris, "Single shot interferometric method for measuring the nonlinear refractive index," OPTICS EXPRESS **21**, 31303-31308 (2013).
11. K. Kitagawa, "Single-shot interferometry without carrier fringe introduction," SPIE **10.1117/2.1201207.004360** (2012).
12. M. Novak, J. Millerd, N. Brock, M. North-Morris, J. Hayes, and J. Wyant, "Analysis of a micropolarizer array-based simultaneous phase-shifting interferometer," APPLIED OPTICS **44**, 6861-6868 (2005).
13. J. C. Wyant, "Advances in interferometric surface measurement," in ICO20: Optical Devices and Instruments (International Society for Optics and Photonics, 2006), pp. 602401-602401-602411.
14. G. Rodriguez-Zurita, N.-I. Toto-Arellano, C. Meneses-Fabian, and J. F. Vázquez-Castillo, "One-shot phase-shifting interferometry: five, seven, and nine interferograms," OPTICS LETTERS **33**, 2788-2790 (2008).
15. P. O'shea, M. Kimmel, X. Gu, and R. Trebino, "Highly simplified device for ultrashort-pulse measurement," OPTICS LETTERS **26**, 932-934 (2001).
16. D. French, C. Dorrer, and I. Jovanovic, "Two-beam SPIDER for dual-pulse single-shot characterization," OPTICS LETTERS **34**, 3415-3417 (2009).
17. R. Trebino, and D. J. Kane, "Using phase retrieval to measure the intensity and phase of ultrashort pulses: frequency-resolved optical gating," JOSA A **10**, 1101-1111 (1993).
18. K. Goda, and B. Jalali, "Dispersive Fourier transformation for fast continuous single-shot measurements," Nature Photonics **7**, 102-112 (2013).
19. C. Gorecki, "Interferogram analysis using a Fourier transform method for automatic 3D surface measurement," Pure Applied Optics **1**, 103-110 (1992).
20. M. A. Hassan, H. Martin, and X. Jiang, "Surface profile measurement using spatially dispersed short coherence interferometry," Surface Topography: Metrology and Properties **2**, 024001 (2014).
21. C. L. Giusca, R. K. Leach, and F. Helery, "Calibration of the scales of areal surface topography measuring instruments: part 2. Amplification, linearity and squareness," Measurement Science and Technology **23**, 065005 (2012).
22. H. Muhamedsalih, F. Gao, and X. Jiang, "Comparison study of algorithms and accuracy in the wavelength scanning interferometry," APPLIED OPTICS **51**, 8854-8862 (2012).

Funding. Ministry of Higher Education and Scientific Research (MOHESR); Engineering and Physical Sciences Research Council (EPSRC) (EP/P006930/1).

Acknowledgment. The author gratefully acknowledge the Department of Laser and Optoelectronics Engineering at the University of Technology, MOHESR, Iraq for funding this work as well as the UK's EPSRC funding for the Future Metrology Hub.